Numerical analysis of thermally induced optical nonlinearity in GaSe layered crystal

E.A.Navarro
M.A.Hernàndez
M.V.Andrés
A.Segura
V.Muñoz

Indexing terms: Numerical analysis, Optical nonlinearity, GaSe layered crystal

Abstract: A numerical approach to studying thermally induced optical nonlinearity in semiconductors is presented. A transient finite difference algorithm is applied to solve the thermal diffusion equation coupled with the nonlinear absorbance–transmittance of Au/GaSe/Au samples with an applied electric field. The presented analysis can deal with any arbitrary axisymmetric dependence of the input power over the sample and external electric field, and provides information about the steady state and transitory effects in the transmittance.

1 Introduction

GaSe layered crystal and Au/GaSe/Au devices constitute Fabry–Perot resonators filled with a nonlinear medium (GaSe). When the GaSe is exposed to an intense laser beam, the refractive index, and then the optical path length of the resonator, changes as a result of the heating, the transmission becomes nonlinear and regions of differential amplification, saturation and hysteresis arise [1, 2]. The Au/GaSe/Au device has also been shown to behave as an optical modulator with relatively low time response. In particular, Iwamura *et al.* [3–5], have reported an anomalously large shift of the absorption edge of 20nm for an applied electric field of 1kV/cm with switching times of the order of 80ns, which may have an excellent application in the modulation of light [3, 4].

In this paper we propose a mathematical model for the analysis of nonlinearity in semiconductors, which takes into account only thermal effects. In our model, the resulting equations are solved by means of a direct numerical procedure, i.e. transient finite differences. The heat diffusion equation is solved in the time domain in combination with optical absorption, photoconductivity and the Joule effect. Numerical results for the transmitted power and switching time are found to be in good agreement with experimental measurements, which confirms that there is no anomalous effect in the layered semiconductor GaSe, as was pointed out by another researchers [6], with exception of the additional heating because of the Joule effect of photoexcited carriers.

© IEE, 1996

IEE Proceedings online no. 19960523

Paper first received 19th January 1996 and in revised form 17th April 1996

The authors are with the Department of Applied Physics, Universitat de València, 46100 Burjassot València, Spain

2 Heat diffusion equation

Transmittance, reflectance and absorbance of the Au/GaSe/Au multilayer can be easily calculated through the matricial model from [7]. The equation governing heat diffusion is:

$$k\nabla^2\theta + \frac{\partial q}{\partial t} = \rho c\frac{\partial \theta}{\partial t} \tag{1}$$

where θ is the temperature, k the material thermal conductivity $\partial q/\partial t = \mathring{q}$ is the heat generation per unit volume and time, ρ the material density, c the specific heat capacity, and t the time.

The sample shape is assumed to be cylindrical with a thickness much smaller than the radius. Thus the longitudinal diffusion is omitted in the numerical model as it is considered to be a very thin layer. The heat generation and the temperature are also assumed to be uniform along the longitudinal axis of the cylindrical thin slab, and the heat losses by convection with air and radiation have been considered negligible.

We assume that a Gaussian laser beam impinges perpendicularly to the surface of the sample. The sources of power in the sample $\mathring{q}$, are the light absorption and the heat that is produced by Joule effect. The applied electric field is assumed to be uniform over the whole sample with the value, $E = V/d$, where V is an applied voltage between the metalised faces of the sample and d is the thickness. The expression for $\mathring{q}$ including these effects is:

$$\mathring{q}(\theta, r) \simeq \left(A_t(\theta) + A(\theta)\frac{e\mu\tau}{h\nu}\frac{V^2}{d^2}\right)\frac{J_o}{d}\exp -\left(\frac{r}{a}\right)^2 + V^2\frac{\sigma^2}{d^2} \tag{2}$$

where the second term in the brackets is due to the Joule effect of photogenerated carriers, $A_t(\theta)$ is the absorption in the whole device, the GaSe and the Au layers, and $A(\theta)$ is the absorption in the GaSe itself. Both absorptions are deducted from the matricial model of [7]. τ and μ are the lifetime and mobility of photogenerated carriers, h is Planck's constant, J_0 the maximum intensity of the laser beam, a is the radius of the laser spot (see Fig. 3), and σ is the conductivity of the material in the dark.

The final expression for eqn. 1 with substituting of eqn. 2 is a nonlinear parabolic equation. Taking into account the shape of the sample, the profile of the laser beam is useful to make use of cylindrical co-ordinates; thus eqn. 1 yields:

$$\frac{1}{r}\frac{\partial}{\partial r}\left(r\frac{\partial\theta}{\partial r}\right)+\frac{P_i}{\pi a^2 kd}\left(A_t(\theta)+\frac{e\mu\tau}{h\nu}\frac{V^2}{d^2}A(\theta)\right)\exp-\left(\frac{r}{a}\right)^2 + V^2\frac{\sigma^2}{kd^2}=\frac{\rho c}{k}\frac{\partial\theta}{\partial r} \quad (3)$$

where $P_i = J_0\pi a^2$ is the incident power.

With the assumption of a very thin sample, we get a nonlinear differential equation dependent only on the radial and time dimensions.

3 Numerical approach

In this Section is outlined a numerical approach to solve eqn. 3 in both time and space dimensions using a direct transient finite difference algorithm.

The temperature in the position $r = i\Delta r$ at the time $t = n\Delta t$ is represented as $\theta(i\Delta r, n\Delta t) = \theta^n(i)$. In this way, a system of equations in finite differences is obtained that can be solved by both explicit or implicit resolution algorithms [8]. The problem that arises with the use of an explicit algorithm is the accumulation of numerical errors and perhaps instability [9]. The time and space increments must be chosen carefully to avoid instability in a explicit finite difference scheme. This is a strong constraint in the choice of Δr and Δt that leads to very small time increments. Because of that, we chose a second way, that is the use of an implicit algorithm. In this case, to obtain the temperature at each point, we have to solve a system of nonlinear equations in which the unknowns are the temperature at each point of the mesh. The advantage of the implicit algorithm is the nonexistence of a constraint over Δr and Δt, and this makes the algorithm faster because we can choose larger Δt. The stability is guaranteed but the accuracy of the numerical results will be dependent on these parameters.

The use of an implicit scheme results in the following system of equations:

$$\frac{\theta^{n+1}(i)-\theta^n(i)}{\Delta t}=\frac{k}{\rho c}\left\{\frac{\theta^{n+1}(i+1)-\theta^{n+1}(i-1)}{i\Delta r^2} + \frac{\theta^{n+1}(i+1)-2\theta^{n+1}(i)+\theta^{n+1}(i-1)}{\Delta r^2}+\frac{\mathring{q}}{k}\right\} \quad (4)$$

for $i = 1$ to N_p, N_p = number of points of the spatial discretisation, where the boundary conditions are,

$$\theta^{n+1}(N_p) = T_{amb} \quad (5)$$

$$\frac{\partial\theta}{\partial r}|_{r=0} = 0 \quad (6)$$

that is, maximum temperature in the centre of the sample and equilibrium temperature in the edge.

In eqn. 4, we use a two-level implicit finite difference scheme that is unconditionally stable, independently of the numerical value of the time and space increments. The finite difference scheme involves six points and is an extrapolated Douglas difference scheme [10] involving the nonlinear term $\mathring{q} = \mathring{q}(\theta^{n+1}, i)$, because these are to be evaluated at the advance level $t = (n + 1)\Delta t$. Since $\theta^{n+1} = \theta^n + O(\Delta t)$ (first-order accuracy in Δt), we modify slightly the difference scheme in eqn. 4, thus $\mathring{q}$ is evaluated at the known level $t = n\Delta t$ so that the resulting algebraic equations at each time step remain linear and can be easily solved by elimination. The error in the calculation of θ^{n+1} is $O(\Delta t, \Delta r^2)$.

However, the application of an iterative process can give a better approach for the nonlinear $\mathring{q}$. The iterative process can be defined by solving the given difference system eqns. 4–6 in the form,

$$L[\theta^{n+1}] = A[\theta^n] + F[\theta^{n+1}] \quad (7)$$

where L and A are linear operators in θ^{n+1} and θ^n, respectively, and $F[\theta^{n+1}]$ is a nonlinear operator involving $\mathring{q}$. We can make use of the Picard process [10]. We replace θ^{n+1} by $\theta^{n+1}[s + 1]$ on the left and by $\theta^{n+1}[s]$ on the operator F. Thus the next approximation $\theta^{n+1}[s + 1]$ is determined by the current approximation $\theta^{n+1}[s]$ by solving the algebraic equations,

$$L[\theta^{n+1}[s+1]] = A[\theta^n] + F[\theta^{n+1}[s]] \quad (8)$$

The 's' parameter in eqn. 8 is the index of iteration in the correcting process for the temperature θ^{n+1}, $\theta^{n+1}[s + 1]$ is obtained from $\theta^{n+1}[s]$ using eqn. 8 for a specific value of 'i'. Thus, the temperature $\theta^{n+1}[s = 1]$ is obtained from eqn. 8 approaching $\theta^{n+1}[s = 0]$ by θ^n. θ^{n+1} [1] is substituted again in eqn. 8 to obtain θ^{n+1} [2], ... θ^{n+1} [s + 1], until convergence is achieved

Following the above procedure, the temperature at every point of the grid that defines the sample is obtained at each time step.

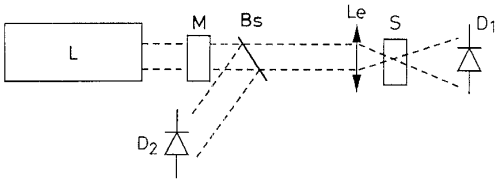

Fig. 1 *Experimental arrangement*
L, Laser, M, Acousto-optical modulator, Bs, beam splitter; Le, Lens; S, sample; D_1, D_2, photodiodes

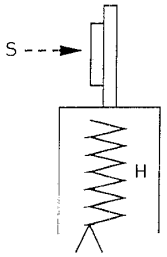

Fig. 2 *Sample holder S, Au/GaSe/Au device; H, heating element*

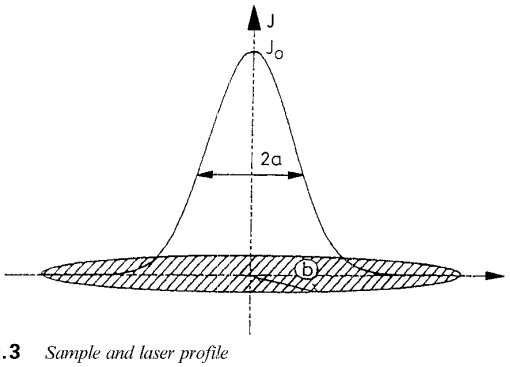

Fig. 3 *Sample and laser profile*

4 Results

Figs. 1–3 show the experimental arrangement for the measurement of the transmitted power versus incident power in an Au/GaSe/Au sample. The temperature

dependence of $A_t(\theta)$ and $A(\theta)$ can be modelled from the temperature behaviour of the refractive index and absorption coefficient. We use the numerical expressions from reference [11] that gives a good fit of refractive index and absorption coefficient to experimental measurements.

First, to show the validity of the numerical technique, a simulation for a Au/GaSe/Au device is performed at stationary conditions with the following parameters and constants corresponding to the laser beam and the device Au/GaSe/Au:

a = 10μm, b = 1.25mm (radius), ρ = 5030kg/m^3, c = 44.66J/mol K + 10^{-5} * θ^{-3} J K^2/mol, k = 16 W/Km, thickness of the GaSe sample d = d(GaSe) = 12.41μm, thickness of the Au deposit d(Au) = 105 Å, σ = 1.5 × 10^{-3} Ω^{-1} cm^{-1}, $e\mu\tau/h\nu$ = 2.0 × 10^7 Å/V^2.

The initial temperature is specified on the whole domain of interest $\theta(i, t = 0) = T_{amb}$, and the applied voltage is defined as well. The temperature at every point of the sample is calculated at each time step $n\Delta t$ following the above iterative process. In that way, the transmitted power is calculated against the incident for a quasistationary slope input power. The obtained numerical results are compared with the experience for different applied voltages V = 0, 8, and 10 volts. Both numerical and experimental results are presented in Fig. 4, and an excellent agreement is observed between our modelling and the measurements.

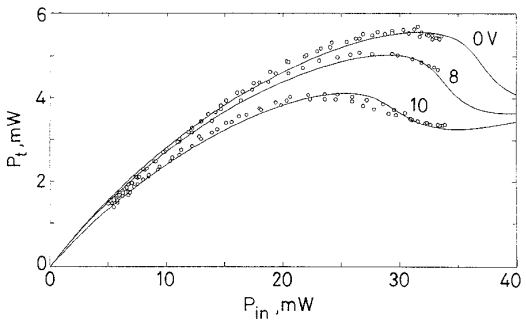

Fig. 4 *Transmitted power, P_t against incident power, P_{in} for different applied electric fields, $E = V/d$) and T_{amb} = 322K*
—— numerical results ◦ experimental results

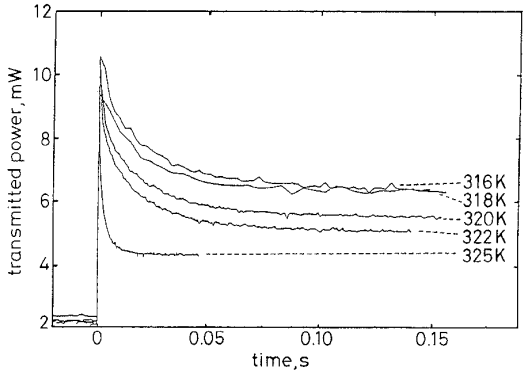

Fig. 5 *Transmitted power against time*
Sample thickness = 12.41μm; incident power is step in time domain, V = 9 volts

An important feature of the Au/GaSe/Au device is its behaviour as a light modulator, giving a modulation very close to 100% of the incident power. The switching time is also an important parameter which is desired to be as short as possible. The switching time is measured from the time in which the laser impinges the Au/GaSe/Au sample until the transmitted power reaches the 90% of its stationary magnitude. The variation of the switching time with the temperature and the applied voltage can be obtained both experimental and numerically with the experimental arrangement of Figs 1–3 and the above numerical procedure. Fig. 5 presents the measured transmitted power versus time for several temperatures and a constant voltage of 9 volts, the incident power is a step in the time of 35mW. Fig. 6 shows the measured transmitted power against time for several applied voltages and a temperature of 322K, the incident power is also a step in the time. In both Figs. 5 and 6 a peak in transmittance appears immediately after turning on the incident light and a later evolution to a state of constant transmission. The steady state in the Au/GaSe/Au device is achieved when the absorbed power equals to the dissipated power. In Fig. 7 is compared the numerically obtained switching time against the measurements for a temperature of 322K.

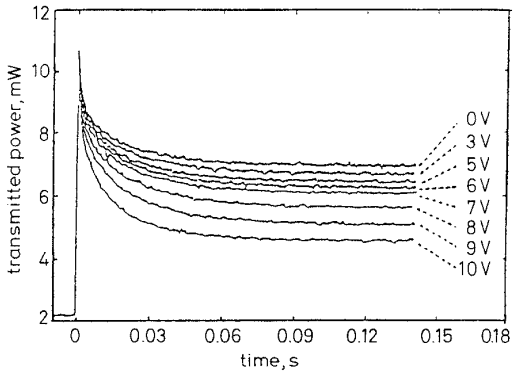

Fig. 6 *Transmitted power against time*
Sample thickness = 12.41μm, incident power is step in time domain, T_{amb} = 322K

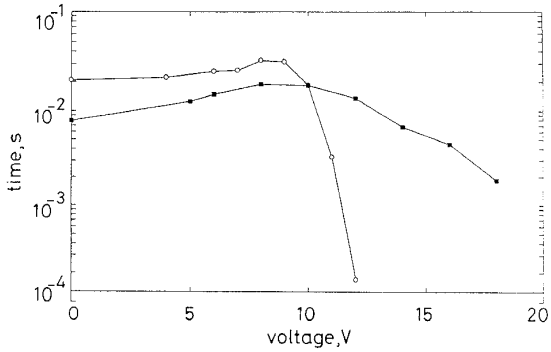

Fig. 7 *Switching time against voltage*
T_{amb} = 322K ◦ experimental results ■ numerical results

The modulation of the transmitted power is possible by applying a square wave voltage. The switching time $\tau\downarrow$, is the time interval from the state of high transmittance until the transmitted power reach the 10% of its stationary value for low transmittance. This time is numerically calculated for some values of the amplitude of a square wave of the applied voltage, the results are presented in Fig. 8, in which they are compared against the experimental values. Since the electrical conductivity σ is not a well known parameter, it scatters a lot for different samples, we think that the difference between numerical and experimental results is caused by a dis-

crepancy in σ. To check this fact we did some simulations for some different σ values to get a better adjust to the measurements. In Fig. 8 are shown results obtained for two of these σ values. It is difficult to fit both numerical an experimental results in the whole voltage range. We can only get a good fit for low amplitudes with $\sigma = 0.0001\ \Omega^{-1}\ cm^{-1}$, or high amplitudes of the applied voltage for $\sigma = 0.0015\ \Omega^{-1}\ cm^{-1}$. We find that the conductivity is sensitive to temperature in the form $\sigma = \sigma_0 \exp(-\gamma/T)$, where γ is an unknown parameter. Thus in the state of high transmittance we have an applied voltage that by the Joule effect gives rise to the temperature and consequently increases σ. For that reason we obtain a good fit with measurements for a higher σ for the higher amplitudes of the voltage. However, for low levels of the applied voltage we get a better match with a lower σ. From [12] it is seen that the ratio $\sigma(T + \Delta T)/\sigma(T) = 15$ is obtained for $T = 322$K and $\Delta T = 25.66$K. This agrees well with the numerical results presented in Fig. 6. In spite of this, a good agreement for the slope is observed in Fig. 8 for both values of σ.

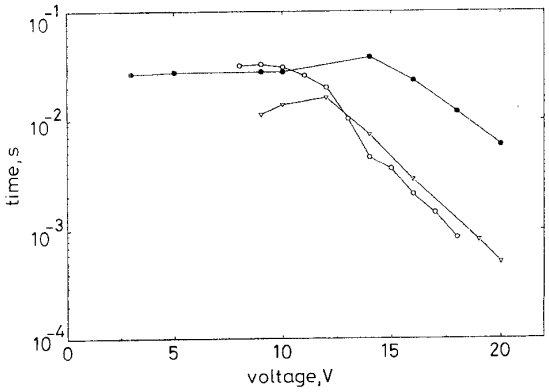

Fig. 8 *Switching time τ↓ against amplitude of square wave voltage*
∘ experimental results; • numerical results with $\sigma = 0.0001\ \Omega^{-1}\ cm^{-1}$; Δ numerical results with $\sigma = 0.0015\ \Omega^{-1}\ cm^{-1}$

5 Conclusion

A nonlinear parabolic equation which describes the operation modes of Au/GaSe/Au devices under the influence of a nonstationary input power and changes in electric applied fields has been presented and numerically solved. This model was used to simulate switching processes in nonlinear devices Au/GaSe/Au, and did show the satisfactory operation mode of the device when it works as an optic modulator of He–Ne laser, showing a switching time about 1 ms. This model explains the device optical nonlinear response as a function of thermal induced effects. We draw the important conclusion that the phenomenon can be explained through purely thermal effects. Both the refraction index and absorption changes with temperature are contributions to nonlinear behaviour. In conclusion, we have shown that the Au/GaSe/Au device exhibits a switching time in the ms range, which is suitable for specific applications to light modulators.

6 References

1 BAKIEV, A.M., DNEPROVSKII, V.S., KOVALYUK, Z.D., and STADNIK, V.A.: 'Optical bistability related to excitons in an uncooled semiconductor', *JETP Lett.*, 1983, **38**, (10), pp. 596–600
2 HERNÁNDEZ, M.A., SÁNCHEZ, J.F., ANDRÉS, M.V., SEGURA, A., and MUNOZ, V: 'Opt. Pur. Apli.', 1993, **26**, pp. 152
3 IWAMURA, Y., MORIYAMA, M., and WATANABE, N.: 'Extended abstracts'. Conference on solid state devices and materials, Sendai, Tokyo, 1990, Sponsored by Business Centre for academic Societies Japan, pp. 617
4 IWAMURA, Y., MORIYAMA, M., and WATANABE, N.: 'Anomalously large shift of absoption edge of GaSe-based layered crystal by applied electric field', *Jap. J. Appl. Phys.*, 1990, **29**, (6), pp. L975–L976
5 IWAMURA, Y., MORIYAMA, M., and WATANABE, N.: 'New light modulator using GaSe layered crystal', *Jap. J. Appl. Phys.*, 1991, **30**, (1A), pp. L42–L44
6 SEGURA, A., ANDRÉS, M.V., and MUNOZ, V.: 'Comments on: anomalously large shift of absoption edge of GaSe-based layered crystal by applied electric field', *Jap. J. Appl. Phys.*, 1991, **30**, (4A), pp. L608–L609
7 MACLEOD, H.A.: 'Thin-film optical filters' (Adam Hilger Ltd, Bristol, 1986)
8 NOUGIER, J.I.: 'Métodes de calcul numérique' (Masson, Paris, 1983), pp. 237–244
9 MIKHLIN, S.G. and SMOLITSKIY, K.L.: 'Approximate methods for solution of differential and integral equations' (Elsevier, New York, 1967), pp. 46–146
10 JAIN, M.K.: 'Numerical solution of differential equations' (Wiley, 1979), pp. 211–312
11 HERNÁNDEZ, M.A., ANDRÉS, M.V., SEGURA, A., and MUNOZ, V.: 'Temperature dependence of refractive index and absorption coefficient of GaSe at 633 nm', *Opt. Commun.*, (to be published)
12 MADELUNG, O., SCHULZ, M., and WEISS, H. (Eds.): 'Landolt–Boernstein tables' (Springer–Verlag, Berlin, Heidelberg, New York, Tokyo, 1983, pp. 293